Role of Electrostatic Interactions in the Binding of Fluorescein by Anti-Fluorescein Antibody 4-4-20†

Vladimir G. Omelyanenko, Wim Jiskoot, and James N. Herron*

Department of Pharmaceutics and Pharmaceutical Chemistry, University of Utah, Salt Lake City, Utah 84112

Received January 25, 1993; Revised Manuscript Received July 15, 1993®

ABSTRACT: Anti-fluorescein antibodies are excellent model systems for studying the biochemical basis of molecular recognition because a prodigious amount of both physico-chemical and structural information is available for these antibodies. Furthermore, recombinant single-chain antibodies have been produced for several anti-fluorescein antibodies, and site-specific mutagenesis studies have defined the energetic contributions of a number of key active-site residues. In previous studies, we determined the three-dimensional structure of an antigen-binding fragment of a high-affinity anti-fluorescein antibody (4-4-20) in complex with fluorescein. These studies showed that fluorescein binds tightly in an aromatic slot and participates in a network of electrostatic interactions. In this report, we examine the role of electrostatic interactions in the 4-4-20 antigen-combining site by observing the effects of pH on the fluorescence of fluorescein and antigen-binding affinity. These studies showed that the salt link between fluorescein and Arg-L34 in 4-4-20 probably accounts for about −1.5 kcal/mol^{-1} of the observed free energy of interaction. Furthermore, at pH 10 and higher, the affinity decreases by more than 100-fold ($\Delta\Delta G^\circ \cong 3$ kcal mol^{-1}). We attributed this decrease to the ionization of Tyr-L32, which probably disrupts a hydrogen bond between tyrosine's hydroxyl group and fluorescein's phenylcarboxylate group. The fluorescence lifetime of the 4-4-20/fluorescein complex was determined at both pH 8 and pH 10.6. Only one lifetime component (0.38 ns) was observed at pH 8, while two components (0.3 and 3.4 ns) were observed at pH 10.6. Titration experiments showed that the longer lifetime component was not due to unbound fluorescein. This led to the hypothesis that at least two conformers exist for the 4-4-20/fluorescein complex at pH 10.6.

In the past five years, the three-dimensional structures of several antibody–antigen complexes have been determined by X-ray crystallography. These structures include complexes of antigen-binding fragments (Fab)[1] with several different antigens and haptens including lysozyme, neuraminadase, peptides derived from myohemerythrin and influenza hemagglutinin, and fluorescein (Fl) [see review articles by Davies *et al.* (1990), Mian *et al.* (1991), and Wilson *et al.* (1991)]. Chothia *et al.* (1989) proposed that at least five of the six complementarity-determining regions (CDR's) exhibit a limited number of main-chain conformations. He attributed this phenomenon to the conservation of a few key residues located in both the CDR loops and framework regions. Conversely, if the backbone conformations of the CDR loops are highly conserved, then specific residues which come into contact with the antigen need to be as multifaceted as possible to accommodate the varied stereochemical and electronic features of the antigen (Mian *et al.*, 1991).

Although crystallographic studies have helped elucidate the structural features of antigen-combining sites, they are not sufficient to fully understand the energetics of antigen–antibody interactions and must be coupled with other techniques to define the individual contributions of each contact residue to overall binding. The energetics of antigen–antibody interactions are dominated by nonbonded forces such as London dispersion forces, electrostatic interactions, and the hydrophobic effect. Conventional wisdom was that the hydrophobic effect would be more important than electrostatic interactions because the ligand could form electrostatic interactions either with the solvent or with the protein (Sturtevant, 1977). However, electrostatic interactions in the interior of a protein may contribute significantly to the interaction energy due to the low dielectric constant found in such environments (Gilson & Honig, 1988).

To date, there have only been a few studies which have examined the energetics of individual contact residues in antigen–antibody complexes. This is because such studies require both structural and thermodynamic information and are usually performed on recombinant antibodies in order to assess the effects of site-specific mutagenesis. Also, anti-hapten antibodies are typically used because it is much easier to measure the antigen-binding affinity for a hapten than for a protein antigen. One such study examined the energetics of key contact residues in a series of recombinant single-chain antibodies (SCA) generated from a monoclonal antibody (4-4-20) which binds Fl (Denzin *et al.*, 1991; Denzin & Voss, 1992). Since the active site of 4-4-20 and other genetically related anti-Fl antibodies (9-40, 12-40, and 5-14) contain hydrophobic, polar, and charged groups (Bedzyk *et al.*, 1990), these antibodies comprise an excellent model system for studying the relative contributions of the hydrophobic and electrostatic effects.

† This work was supported in part by PHS Grant No. AI 22898 (J.N.H.); a NATO Science Fellowship awarded by NWO, the Dutch Organization for Scientific Research (W.J.); and the Center for Biopolymers at Interfaces.

® Abstract published in *Advance ACS Abstracts,* September 15, 1993.

[1] Abbreviations: Arg, arginine; CDR, complementarity-determining region; SCA, recombinant single-chain antibody; Fab, antigen-binding fragment; Fl, fluorescein; Fl-to-site ratio, mole ratio of fluorescein to antigen-combining sites; H_3, third complementarity-determining region of the heavy chain; His, histidine; HPF, 6-hydroxy-9-phenylfluoron; Mab, monoclonal antibody; ns, nanoseconds; Q_{max}, maximum quenching constant for anti-Fl antibodies; Ser, serine; τ, fluorescence liftetime; Trp, tryptophan; Tyr, tyrosine; MPD, 2-methyl-2,4-pentanediol; PEG, poly(ethylene glycol); χ^2, chi square.

0006-2960/93/0432-10423$04.00/0

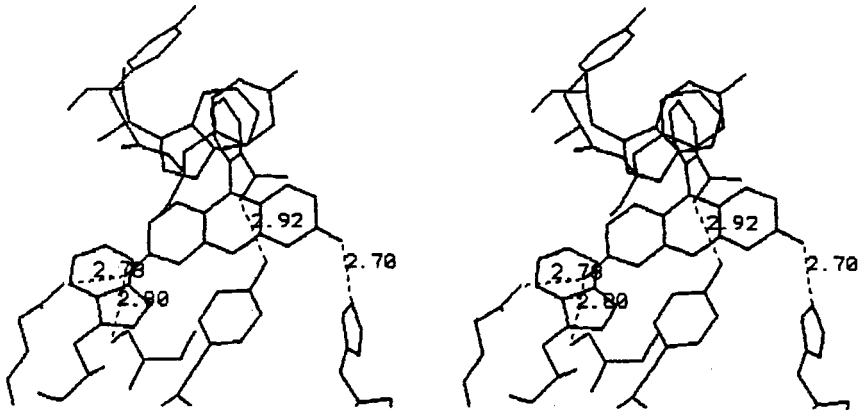

FIGURE 1: Stereoview of the antigen-combining site of anti-Fl antibody 4-4-20. The following contact residues are shown: (bottom: from left to right) Arg-L34, Trp-L96, Ser-L91, Tyr-L32, His-L27d; (top: fore, left, rear) Tyr-H97, Tyr-H96, Trp-H33. Fluorescein is located in the center.

The three-dimensional structure of the 4-4-20 Fab/Fl complex was determined in our laboratory and indicated that Fl binds tightly in an aromatic slot and participates in a network of electrostatic interactions (Herron *et al.*, 1989, 1993). The aromatic slot is formed by Trp-L96 at its base and Trp-H33 and Tyr-L32 on the sides (see Figure 1). The width of the slot is about 9 Å, as measured between the centroids of the rings of Trp-H33 and Tyr-L32. The phenolic ring of Tyr-L32 is stacked with the xanthenone group of Fl. The electrostatic network consists of three hydrogen bonds and a salt link: (1) a hydrogen bond between NE_2 of His-L27d and O_1 of Fl, (2) a hydrogen bond between OG of Ser-L91 and O_3 of Fl, (3) a hydrogen bond between OH of Tyr-L32 and O_5 of Fl, and (4) a salt link between NH_2 of Arg-L34 and O_3 of Fl.

In this paper, we use fluorescence spectroscopy to probe the strength of two of the above interactions: the salt link between Arg-L34 and Fl's enolic group and the hydrogen bond between Tyr-L32 and Fl's phenylcarboxylate group. In the first case we examined the ionization state of the enolic group of the Fl hapten, while in the second case we examined the pH dependence of the dissociation constant. We also studied the conformation of the active site after the ionization of the phenolic group of Tyr-L32 using time-resolved fluorescence spectroscopy. These results are compared to those obtained by chain reassociation studies and site-specific mutagenesis studies (Bedzyk & Voss, 1991; Bedzyk *et al.*, 1992; Denzin *et al.*, 1991).

MATERIALS AND METHODS

Preparation of Mabs. Anti-Fl Mabs 4-4-20 and 9-40 were generated through chemically mediated fusion of BALB/c splenic lymphocytes with the Sp 2/0-Ag 14 myeloma cell line as described by Kranz and Voss (1981). Hybridoma cell lines were obtained from Prof. Edward W. Voss, Jr. (University of Illinois at Urbana–Champaign). Mabs were purified by ammonium sulfate precipitation followed by DEAE-cellulose anion exchange and chromatofocusing over a pH gradient of 7.0 to 5.0. Preparations were characterized by gel electrophoresis and fluorescence quenching assays (Herron, 1984). Antibody solutions were filtered through Durapore 0.2-μm filters (Millipore Corporation, Bedford, MA) before use.

Measurement of the Ionization Constant (pK_a) by Fluorescence Spectroscopy. Antibody solutions were prepared in 50 mM potassium phosphate with 50 mM potassium chloride (pH 8.0) and then adjusted to different pH values with 0.5 M hydrochloric acid or 0.5 M sodium hydroxide. An IgG concentration of 4×10^{-6} M and a Fl concentration of 10^{-7} M were used in all experiments. Fluorescence measurements were made using a photon-counting spectrofluorometer (Model PC-1, ISS, Champaign, IL). Samples were excited at 485 nm for free Fl and at 500 nm for bound Fl using a monochromator with a 2-mm slit width (8 nm/mm fwhm band-pass), and emission was monitored at 540 nm, using a monochromator with a 2-mm slit width (8 nm/mm fwhm band-pass). Furthermore, a 515-nm cut-on filter was used to eliminate light scatter. Temperature was controlled at 25 °C with a circulating water bath. The pK_a value was computed using eq 1:

$$F = \frac{\lim_1 + \lim_2 10^{(pH-pK_a)}}{1 + 10^{(pH-pK_a)}} \quad (1)$$

where F is the fluorescence of a pH-sensitive fluorophore, $\lim_1$ is the limiting fluorescence of the fluorophore at low pH, and $\lim_2$ is the change in fluorescence during the course of a pH titration.

Affinity Determination. The antigen-binding affinities of 4-4-20 and 9-40 were measured using a fluorescence quenching assay described by Herron (1984). In brief, an initial volume of 2 mL of antibody (at an optimum concentration for determining the affinity of the protein) was added to a fluorescence cuvette and small aliquots of Fl solution were added. In order to maintain a relatively constant protein concentration, the total volume of Fl solution added was less than 0.05 mL. Samples were prepared in either 50 mM glycine buffer or 50 mM potassium phosphate buffer (each with 50 mM potassium chloride), depending on the pH value. All experiments were performed at 25 °C.

The dissociation constant (K_d) was determined using the following equation:

$$K_d = \frac{(1 - f_b)(NP_0 - f_b C_0)}{f_b} \quad (2)$$

where f_b is the fraction of bound Fl, N is the antibody valence, and P_0 and C_0 are total concentrations (bound + free) of antibody and ligand, respectively. The fraction of bound Fl was determined from fluorescence quenching data using eq 3:

$$f_b = Q/Q_{max} \quad (3)$$

where Q is the fluorescence quenching of a given mixture of antibody and Fl, and Q_{max} is the maximum fluorescence quenching of Fl observed when 100% of the ligand is bound.

Calculation of Coupling Free Energy. If the ionization of an acidic or a basic group is coupled to some other interaction such as the formation of a hydrogen bond or a salt link, then the total free energy (ΔG_{tot}) of the ionization reaction (HA $\rightleftharpoons$ $H^+ + A^-$)is given by eq 4:

$$\Delta G_{tot} = \Delta G_{ioniz} + \Delta G_c \quad (4)$$

where ΔG_{ioniz} is the ionization energy, and ΔG_c is the coupling free energy. The ionization energy is given by equation 5:

$$\Delta G_{ioniz} = \Delta G^\circ + RT \ln\left\{\frac{[H^+][A^-]}{[HA]}\right\} \quad (5)$$

If the system is allowed to reach equilibrium ($\Delta G_{tot} = 0$), then the hydrogen ion concentration at which the acid is half-ionized is given by

$$[H^+]_{1/2} = e^{-((\Delta G^\circ + \Delta G_c)/RT)} \quad (6)$$

and the apparent pK_a' is

$$pK_a' = -\log[H^+]_{1/2} = (\Delta G^\circ + \Delta G_c)/2.303RT \quad (7)$$

For free Fl in aqueous solution, there is no coupling, and the pK_a is given by

$$pK_a = \frac{\Delta G^\circ}{2.303RT} \quad (8)$$

Therefore, the coupling energy can be computed from the difference in the two pK_a values:

$$\Delta G_c = 2.303RT(pK_a' - pK_a) \quad (9)$$

Fluorescence Lifetime Measurements. Lifetime measurements were performed using a multifrequency phase and modulation fluorometer (Model K2, ISS, Champaign, IL). Samples were excited using the 488-nm line of an argon-ion laser (Model 2045, Spectra Physics, Mountain View, CA) through an excitation polarizer set at vertical position (0°). Emission was monitored through a 530-nm cut-on filter and an emission polarizer set at 55°. A solution of Fl (pH 8.0) was used as a fluorescence lifetime reference (lifetime τ = 3.95 ns) for all measurements. Phase and modulation data were collected at 15 frequencies between 10 and 200 MHz. The temperature of the sample chamber was maintained at 25 °C with a circulating water bath. For each frequency, fluorescence lifetime measurements were taken until the phase angle and modulation ratio errors were less than or equal to 0.2° and 0.004, respectively. Measurements were done in triplicate, and the phase and modulation data were averaged prior to analysis. Data were analyzed using Global Unlimited analysis software (Beechem & Gratton, 1988), and the best fits were obtained for discrete exponential fluorescence lifetimes.

RESULTS AND DISCUSSION

Ionization Constant (pK_a) of Enolic Groups of Fl. Fluorescein may exist in several different ionic forms: (I) a cation with a positive charge localized in the xanthenone ring, (II) a neutral molecule, (III) a monoanion with a negatively charged phenylcarboxylate group (pK_a = 4.4), and (IV) a dianion when one of the enolic groups (O_1 or O_3) is deprotonated (see Figure 2). The absorption spectra of these forms have previously been measured in aqueous solution and exhibit the following absorption maxima: (1) 437 nm for the cation, (2) 437 nm for the neutral form, (3) 475 for the monoanion, and (4) 492 nm for the dianion. The fluorescence emission spectra of all four forms have similar shapes (Martin & Lindqvist, 1975), but the dianionic form has a much higher quantum yield of fluorescence than the monoanionic, neutral, and cationic forms.

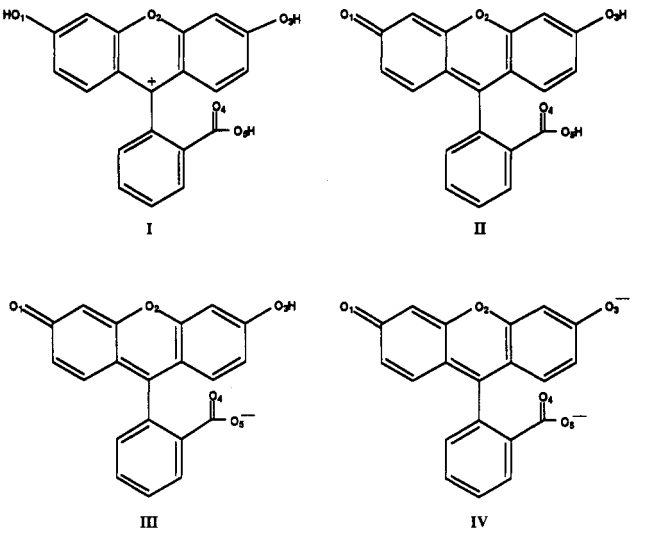

FIGURE 2: The four ionic forms of Fl: (I) cation, (II) neutral molecule, (III) monoanion, and (IV) dianion.

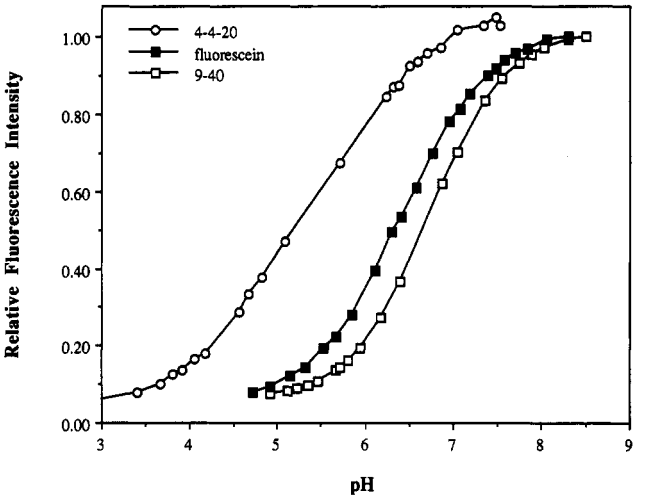

FIGURE 3: pH dependence of the fluorescence intensity of (○) Fl/4-4-20 complex, (■) free Fl, and (□) Fl/9-40 complex. An antibody concentration of 4×10^{-6} M was used in the first and third experiments. The same concentration of Fl (10^{-7} M) was used in all three experiments. Excitation wavelengths of 485 and 500 nm were used for free and bound Fl, respectively.

As a prelude to determining the pK_a value of the Fl/antibody complex, we determined the pK_a of free Fl by plotting its fluorescence intensity versus pH. Because of the different ionic forms of Fl, there was a question of what excitation wavelength to use. Previous studies had shown that Fl exhibits the spectral properties of the dianionic species when bound to 4-4-20 (Kranz *et al.*, 1982), so samples were excited both at 500 nm and at the isosbestic point of the mono- and dianionic species (457 nm). The emission spectra recorded at the two excitation wavelengths were identical. The fluorescence intensity as a function of pH obtained with 500-nm excitation is shown in Figure 3. A pK_a value of 6.35 ± 0.1 was calculated for the enolic group from this titration curve. This was lower than the value of 6.7 measured by Martin and Lindqvist (1975) for the pK_a of Fl's enolic group. We discovered that this discrepancy was due to the presence of 50 mM potassium chloride in our buffer system. When the experiment was repeated in HEPES buffer without salt, a pK_a value of 6.65 ± 0.05 was obtained.

Interaction of Fl with Arg-L34. The crystal structure of 4-4-20 showed that one of Fl's enolic groups (O_3) is sufficiently close (2.8 Å) to Arg-L34 to form a salt link (Herron *et al.*, 1989, 1993). Furthermore, site-specific mutagenesis experiments with single-chain derivatives of 4-4-20 have demonstrated that Arg-L34 (when changed to His) was responsible for a decrease in affinity (Denzin *et al.*, 1991). This result indicated that the electrostatic interaction between Arg-L34 and Fl's enolic group is an important component of 4-4-20's high antigen binding affinity. Considering the high ionization constant of Arg ($pK_a \cong 12$), the electrostatic interaction between Arg-L34 and Fl is expected to change the pK_a of the enolic group. To investigate this possibility, we examined the fluorescence intensity of the Fl/4-4-20 complex as a function of pH (Figure 3). This experiment was repeated with another anti-Fl antibody (9-40) which is very similar to 4-4-20 except that it has a His residue at position L34 instead of Arg, as well as several differences in the third CDR of the heavy chain (H_3) (Bedzyk *et al.*, 1990).

As can be seen in Figure 3, a considerable shift occurs in the titration curve for liganded Fl compared to that of free Fl. The curve for 4-4-20 is shifted to the acidic side, while that of 9-40 is shifted in the opposite direction. The pK_a values calculated from these curves are 5.2 ± 0.1 for the Fl/4-4-20 complex and 6.7 ± 0.1 for the Fl/9-40 complex. In the case of 4-4-20, there are two electrostatic interactions with Fl's enolic group: a hydrogen bond with Ser-L91 and a salt link with Arg-L34. Since the guanidino group of the Arg has a high ionization constant, it will be positively charged in the antigen-combining site. This will cause the enolic group of bound Fl to deprotonate at a lower pH than in bulk solution.

The explanation for the increase in pK_a observed for 9-40 is less clear because the crystal structure of 9-40 has not yet been determined. As mentioned above, the primary sequences of the two antibodies differ at position L34 (Arg in 4-4-20, His in 9-40) and also in the third CDR of the heavy chain (SYYGMDY in 4-4-20, YGYHGAY in 9-40). We have used molecular modeling to change the three-dimensional structure of the 4-4-20 antigen-combining site into that of 9-40. These studies showed that His-L34 is about 3.5 Å from Fl's enolic group, so it probably does not form a hydrogen bond. However, Ser-L91 is positioned adjacent to Fl's enolic group in both 4-4-20 and 9-40 and probably forms a hydrogen bond in both cases. Although our molecular modeling studies left some uncertainties about the exact conformation of 9-40's H_3 loop, in one of the possible conformations the imidazolium group of His-H98 was adjacent to Fl's enolic group. In this position, it could readily form a hydrogen bond. If this indeed is the case, the monoanionic form of Fl would probably be favored in the antigen-combining site because its extra hydrogen atom would provide more flexibility in forming hydrogen bonds. This would have the effect of shifting the pK_a of the enolic group to a higher value.

As mentioned above, the pK_a of Fl's enolic group shifts from 6.3 to 5.2 upon binding to 4-4-20. Using eq 9, this gives a coupling free energy of about −1.5 kcal/mol, presumably for the formation of the salt link between Arg-L34 and Fl's enolic group. Since the free energy of binding is about −13.5 kcal/mol for the Fl/4-4-20 complex, this electrostatic interaction accounts for about 11% of the binding energy. Interestingly, similar calculations for 9-40 gave a coupling free energy of about 0.5 kcal/mol, which implies that, in the case of 9-40, electrostatic interactions with Fl's enolic group are somewhat unfavorable.

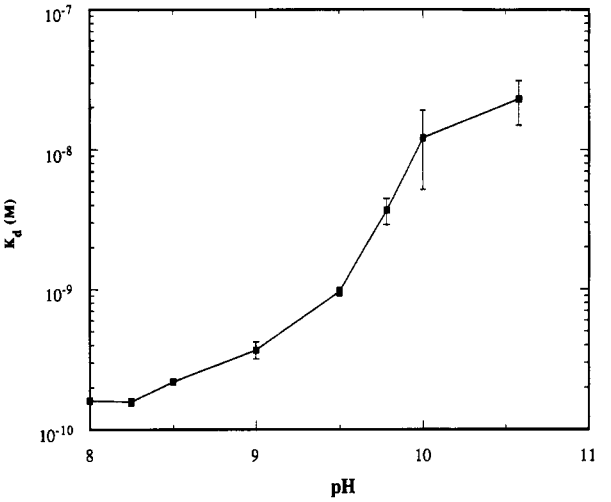

FIGURE 4: pH dependence of the dissociation constant of the Fl/4-4-20 complex. Dissociation constants were determined at each pH value using a fluorescence quenching assay that was described previously (Herron, 1984).

Interaction of Fl with Tyr-L32. Fluorescein's second negative charge is located on its phenylcarboxylate group (O_5, Figure 2). This group's pK_a is about 4.5, and it forms a hydrogen bond with the hydroxyl group of Tyr-L32 (Herron *et al.*, 1993). The pK_a of Tyr's hydroxyl group is usually between 9.6 and 10.0 (Cantor & Schimmel, 1980). Thus, electrostatic repulsion is expected between Fl and Tyr-L32 at pH 10 and above. This should result in a decrease in affinity. We tested this hypothesis by measuring the dissociation constant (K_d) of the Fl/4-4-20 complex over a pH range of 8–11. These data are shown in Figure 4. The K_d increases from 1.6×10^{-10} M at pH 8.0 to 2.3×10^{-8} M at pH 10.6. The midpoint of the transition occurs at about pH 9.7, very close to the expected pK_a value of Tyr's hydroxyl group. Over this pH range, the standard free energy ($\Delta G°$) for the formation of the Fl/4-4-20 complex increases (becomes less favorable) by ca. 3 kcal/mol.

Presumably, this decrease in affinity is due to electrostatic repulsion between Fl and Tyr-L32, although other factors such as the deprotonation of lysine residues may also be implicated at elevated pH values. Recent studies have shown that the conformation of the antibody molecule as a whole does not change significantly between pH 8 and 10 (Buchner *et al.*, 1991; Jiskoot *et al.*, 1991). So, it is unlikely that the observed decrease in affinity is due to denaturation. It is informative to compare our results to a site-specific mutagenesis study by Denzin and Voss (1992) in which position L32 of a single-chain derivative of 4-4-20 was changed from Tyr to Phe. In this case, an increase in standard free energy ($\Delta\Delta G°$) of 1.8 kcal/mol was observed. This value probably reflects the electrostatic energy between Tyr's hydroxyl group and Fl's phenylcarboxyl group. The greater free energy change ($\Delta\Delta G°$) observed in our case may result from a change in the conformation of the antigen-combining site in addition to the loss of the electrostatic interaction (see below).

Hydroxyphenylfluoron (HPF) is an analog of Fl that does not contain the carboxylic acid group on the phenyl ring. Recently, Bedzyk *et al.* (1992) showed that the standard free energy ($\Delta G°$) of the HPF/4-4-20 complex was 2.9 kcal/mol higher (less favorable) than that of the Fl/4-4-20 complex at 20 °C. Presumably, this difference reflects the contribution to binding of the phenylcarboxylate group. However, there are probably several other factors in addition to the electrostatic interaction. Most notably, HPF exhibits much greater

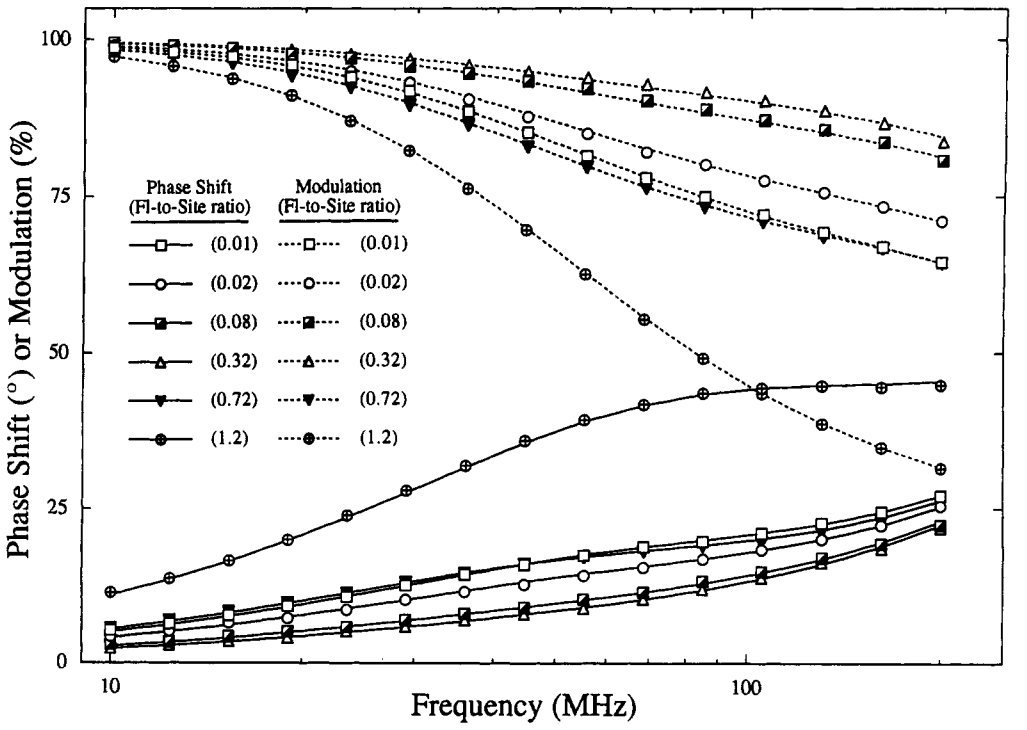

FIGURE 5: Fluorescence lifetime measurements for the 4-4-20/Fl complex at pH 10.6. The ratio of Fl to antigen-combining sites (Fl-to-site ratio) was varied over the range 0.01–1.2, and fluorescence lifetime measurements were taken at each ratio. Phase-shift and demodulation values were plotted versus modulation frequency for the following Fl-to-site ratios: (□) 0.01, (○) 0.02, (◪) 0.08, (△) 0.32, (▼) 0.72, and (⊕) 1.2. Measurements were also taken for ratios of 0.04 and 0.16, but for the sake of clarity, these data are not shown. Phase and modulation data were analyzed using Globals Unlimited (Beechem & Gratton, 1988), and the results are presented in Table I and Figure 6. The solid lines represent the theoretical fits for the three-component model.

torsional flexibility of its phenyl ring relative to the xanthenone ring than observed for Fl. This should result in some loss in configurational entropy upon binding. Furthermore, since the antigen-combining site was designed to accommodate the phenylcarboxylate group, the absence of this group in HPF will result in fewer van der Waals contacts.

Influence of Tyr-L32 on the Maximum Quenching Constant (Q_{max}). In addition to its antigen-binding affinity, each anti-Fl Mab exhibits a unique maximum quenching value (Q_{max}), which is defined as the fluorescence quenching of a totally bound population of Fl. The reported Q_{max} value of 4-4-20 is about 95% (Herron, 1984), but it can vary somewhat depending on the optical geometry of the fluorometer. Until recently, it was unclear which residues were responsible for quenching Fl's fluorescence. This matter has been clarified to some degree by the aforementioned study by Denzin and Voss (1992) which showed that a mutation of L34 from Arg to His reduced the Q_{max} value of the 4-4-20 SCA to 28%, but mutation of L32 from Tyr to Phe had almost no effect. In our pH studies, we observed a Q_{max} value of 98% at pH 8.0 and a value of 97% at pH 10.6. Thus, our results are consistent with Denzin and Voss's observation that L32 does not seem to be involved in fluorescence quenching. Several workers have also suggested that Trp is partially responsible for the quenching of Fl in anti-Fl antibodies (Watt & Voss, 1977; Templeton & Ware, 1985). In 4-4-20 there are two Trp residues (L96 and H33) which are in van der Waals contact with Fl (see Figure 1). To date, the role of these residues in the quenching mechanism of fluorescein has not been directly probed, but it is conceivable that they account for part of the residual quenching observed when L34 was changed from Arg to His.

Lifetime of Bound Fl at Elevated pH Values. One way to probe the environment of the antigen-combining site is to measure the lifetime of bound Fl. Conformational changes in the antigen-combining site at elevated pH values may significantly affect the orientation of Fl and hence its lifetime. Fluorescence lifetime measurements were made at pH 8.0 and 10.6. A single fluorescence lifetime of 3.95 ns was found for free Fl at both pH values. In addition, a single lifetime value of 0.38 ±0.02 ns was observed for bound Fl at pH 8.0. However, two components were found for bound Fl at pH 10.6 (0.31 ± 0.01 and 3.40 ± 0.08 ns). Although this measurement was taken in the presence of a large molar excess (100-fold) of antigen-binding sites to Fl, it was conceivable that the longer lifetime component was due to the presence of a small amount of free (unbound) Fl that had dissociated at pH 10.6.

In order to investigate this possibility, the antibody solution was titrated with Fl; specifically, the ratio of Fl to antigen-binding sites (Fl-to-site ratio) was varied from 0.01 to 1.2, and fluorescence lifetime measurements were taken at each ratio. These data are presented in Figure 5 and show that the average fluorescence lifetime decreased with increasing Fl-to-site ratio. This result was inconsistent with the hypothesis that the longer lifetime component (3.4 ns) was due to free Fl. In fact, two-component analyses of these data showed that the fractional contribution of the shorter lifetime component (0.31 ns) increased upon addition of Fl, rather than that of the longer lifetime component (3.4 ns). This trend continued until the antibody was nearly saturated with Fl (Fl-to-site ratio = 0.72; see Figure 5), at which point the longer lifetime component changed from 3.40 to 3.95 ns. Finally, as the Fl-to-site ratio was increased from 0.72 to 1.2, the fractional contribution of the longer lifetime component increased to reflect the increasing amount of free Fl. Thus, it appeared that three lifetime components were present at pH 10.6: a 0.31-ns component due to bound Fl, a 3.4-ns component that was more prevalent at low Fl-to-site ratios and was probably due to another bound species of Fl, and a

Table I: Global Analysis of Phase and Modulation Data for the Fl/4-4-20 Complex at pH 10.6[a]

τ_1 (ns)	τ_2 (ns)	τ_3 (ns)	range of individual reduced χ^2 values[b]	global reduced χ^2
Two-Component Model				
0.32 [0.30–0.33]	3.9 [3.8–4.1]		1.04–6.61	2.59
0.32 [0.31–0.33]	3.95 (F)[c]		1.05–6.63	2.58
Three-Component Model				
0.31 [0.30–0.32]	3.4 [3.3–3.6]	4.1 [3.9–5.1]	0.29–1.25	0.69
0.30 [0.30–0.31]	3.4 [3.3–3.6]	3.95 (F)[c]	0.27–1.21	0.92

[a] The ratio of Fl to antigen-combining sites (Fl-to-site ratio) was varied over the range 0.01–1.2, and fluorescence lifetime measurements were taken at each ratio. A total of eight data sets were obtained. Phase-shift and demodulation data (see Figure 5) were analyzed using Globals Unlimited (Beechem & Gratton, 1988). Two different models were evaluated: (1) a two-component model which contained lifetime components for free (3.94 ns) and bound (0.32 ns) Fl and (2) a three-component model which contained an additional lifetime component (3.4 ns) which probably represents another conformer of the Fl/4-4-20 complex. The data in brackets represent the confidence intervals at the 98% level, as obtained from correlated error analysis using Globals Unlimited. [b] Range of reduced χ^2 values observed for the eight individual data sets (obtained at different Fl-to-site ratios). Please note that the χ^2 values for the individual data sets are significantly lower for the three-component model than for the two-component model; the estimated errors used for the phase and modulation data are 0.2° and 0.004, respectively; χ^2 values smaller than 1 indicate that the actual errors were smaller than the estimated ones in some of the data sets. [c] Fluorescence lifetime value fixed to that of free Fl.

3.95-ns component that was only observed at high Fl-to-site ratios and was probably due to free Fl.

Global analysis (Beechem & Gratton, 1988) was used to distinguish between this three-component model and a more traditional two-component model that contained a 0.32-ns component for bound Fl and a 3.95-ns component for free Fl. Specifically, the lifetimes of the individual data sets were linked and the fractional intensities were allowed to vary. These data are presented in Table I. The three-component model fitted the data better than the two-component model, as evidenced by the significant reduction in the chi-square values (χ^2) observed in the former case (global reduced χ^2: 0.69 for the three-component model, 2.59 for the two-component model). Rigorous error analysis, in which a complete minimization for each fixed value of the tested parameter was performed using the Globals Unlimited software, showed that the 3.4-ns and 3.95-ns lifetimes were significantly different at the 98% confidence level. Moreover, in the case of a two-component fit, the fraction of the 3.95-ns component initially decreased with increasing Fl-to-site ratio (data not shown), which would be difficult to explain if the long-lifetime component was due to free Fl. Figure 6 shows the fractional intensities for the three-component model. The fractional intensity of the 3.4-ns component gradually decreased with the addition of Fl, while the free Fl component (3.95 ns) only appeared at high Fl-to-site ratios.

Our interpretation of these results is that there are two conformations of the Fl/4-4-20 complex at pH 10.6: (i) a "tight" conformation that has a short fluorescence lifetime (ca. 0.3 ns) and is very similar to the standard conformation observed at pH 8; and (ii) a "relaxed" conformation that has a longer fluorescence lifetime (ca. 3.4 ns), which is probably due to less stringent interactions between Fl and residues in the antigen-combining site that are responsible for fluorescence quenching. Our results indicate that as more Fl is added to the antibody, it binds preferentially to the tight conformer, presumably because this conformer has a higher affinity than the relaxed conformer. Eventually, after both conformers are saturated, a significant amount of unbound Fl with a lifetime of 3.95 ns is present.

Previous kinetic studies with 4-4-20 and other anti-Fl antibodies showed that a two-step mechanism was involved in the binding of Fl (Kranz *et al.*, 1982; Herron, 1984). Two conformers were observed in these studies, one with a Q_{max} value of about 70% and a second with a Q_{max} value of 96%. Fluorescein bound initially to the conformer with the lower Q_{max} value, and then the complex slowly changed into the conformer with the higher Q_{max} value. Second-order kinetics were observed for the formation of the complex, while first-order kinetics were observed for the interconversion process (Kranz *et al.*, 1982). This mechanism is consistent with our

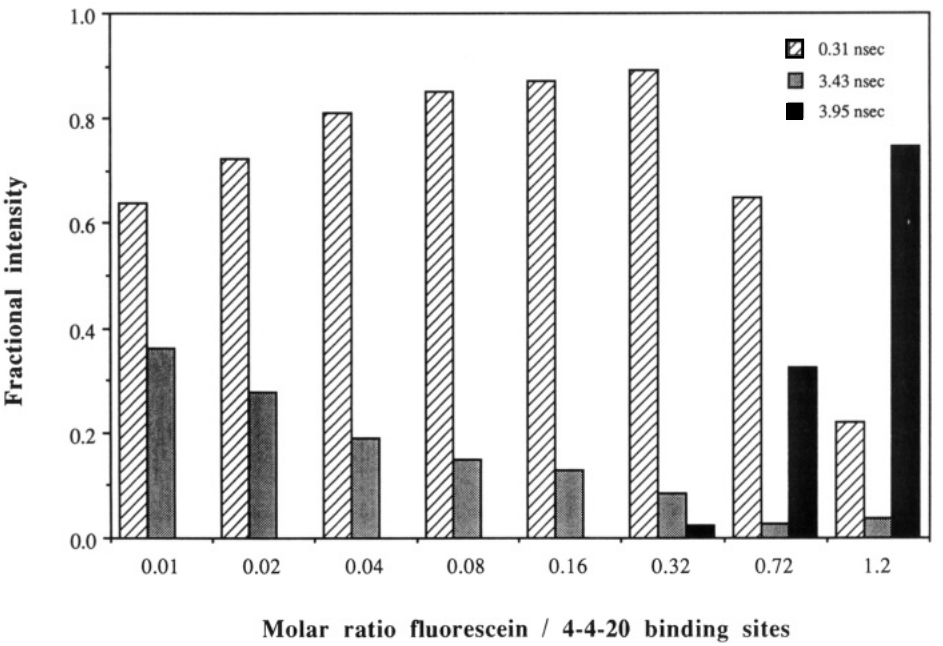

FIGURE 6: Fractional intensities of the three lifetime components of the Fl/4-4-20 complex at pH 10.6. Phase and modulation data presented in Figure 5 were analyzed using Globals Unlimited. Both two- and three-component models were evaluated, and the latter produced a more convincing fit (see Table I). The fractional fluorescence intensities of the three components are plotted versus the Fl-to-site ratio.

lifetime measurements at pH 10.6. The 3.4-ns component was most discernible at low Fl-to-site ratios, and its fraction decreased as more Fl was added (see Figure 6). Because of its longer fluorescence lifetime, this component is also expected to have a lower Q_{max} value than the 0.3-ns component. Thus, the relaxed conformer may actually be an intermediate step or transition state in the binding reaction. This possibility will be investigated in future studies.

CONCLUSIONS

The role of electrostatic interactions in the formation of the Fl/4-4-20 complex was investigated by observing the effects of pH on antigen-binding affinity and the fluorescence of Fl. These studies showed that the salt link between fluorescein and Arg-L34 probably accounts for about −1.5 kcal/mol of the observed free energy of interaction. Furthermore, at pH 10.6, the affinity decreased by more than 100-fold ($\Delta\Delta G^\circ \cong$ 3 kcal/mol). This decrease was attributed to the ionization of Tyr-L32, which probably disrupts a hydrogen bond between Tyr's hydroxyl group and Fl's phenylcarboxylate group. Both of these observations were consistent with $\Delta\Delta G^\circ$ values determined by site-specific mutagenesis studies of the 4-4-20 single-chain antibody (Denzin *et al.*, 1991; Denzin & Voss, 1992). Taken together, these electrostatic interactions account for −4.5 kcal/mol. Although this value is significantly less than the observed free energy of formation for the Fl/4-4-20 complex (ca. −13.5 kcal/mol), it probably represents a major portion of the electrostatic contribution to the free energy change (ΔG°_{elec}).

Several workers have suggested that the free energy change observed for protein folding or complex formation is related to the surface area of nonpolar groups which are buried inside the folded protein or the protein/ligand complex (Sharp *et al.*, 1991). Typically, a conversion factor of −25 cal mol^{-1} Å^{-2} is used to relate buried, non-polar surface area to free energy, although literature reports of this value vary over a range of −16 to −31 cal mol^{-1} Å^{-2} (Sharp *et al.*, 1991). In the case of 4-4-20, about 350 Å^2 of nonpolar surface area is buried upon formation of the Fl/4-4-20 complex (Herron *et al.*, 1993). Using the above conversion factor, this gives a free energy change of ca. −8.8 kcal/mol. We view this value as the hydrophobic contribution to the free energy change (ΔG°_{hydro}). Interestingly, the sum of the electrostatic and hydrophobic contributions ($\Delta G^\circ_{elec} + \Delta G^\circ_{hydro} = -13.3$ kcal/mol) comes very close to the observed free energy of formation for the Fl/4-4-20 complex.

Recent studies have shown that a significant amount of surface area is buried upon formation of antigen–antibody complexes (Davies *et al.*, 1990). In addition, hydrogen bonds and salt links between buried groups were observed in many of these complexes. Such electrostatic interactions may be significantly stronger than comparable interactions in bulk solvent because of the low dielectric constant within the binding cavity (Gilson & Honig, 1988). On the basis of these considerations, we propose that high-affinity antigen-binding sites can be constructed by adding a few key electrostatic interactions to a hydrophobic binding cavity. This is certainly true in the case of 4-4-20 and may be of applicability to the antigen–antibody complexes in general.

REFERENCES

Bedzyk, W. D., & Voss, E. W., Jr. (1991) *Mol. Immunol. 28*, 27–34.

Bedzyk, W. D., Herron, J. N., Edmundson, A. B., & Voss, E. W., Jr. (1990) *J. Biol. Chem. 265*, 133–138.

Bedzyk, W. D., Swindlehurst, C. A., & Voss, E. W., Jr. (1992) *Biochim. Biophys. Acta 1119*, 27–34.

Beechem, J. M., & Gratton, E. (1988) *Proc. SPIE-Int. Soc. Opt. Eng. 909*, 70–81.

Buchner, J., Renner, M., Lilie, H., Hinz, H.-J., Jaenicke, R., Kiefhaber, T., & Rudolph, R. (1991) *Biochemistry 30*, 6922–6929.

Cantor, C. R., & Schimmel, P. R. (1980) *Biophysical Chemistry, Part I: The conformation of biological macromolecules*, p 45, W. H. Freeman and Company, New York.

Chothia, C., Lesk, A. M., Tramontano, A., Levitt, M., Smith-Gill, S. J., Air, G., Sheriff, S., Padlan, E. A., Davies, D., Tulip, W. P., Colman, P. M., Spinelli, S., Alzari, P. M., & Poljak, R. J. (1989) *Nature 342*, 877–883.

Davies, D. R., Padlan, E. A., & Sheriff, S. (1990) *Annu. Rev. Biochem. 59*, 439–473.

Denzin, L. K., & Voss, E. W., Jr. (1992) *J. Biol. Chem. 267*, 8925–8931.

Denzin, L. K., Whitlow, M., & Voss, E. W., Jr. (1991) *J. Biol. Chem. 266*, 14095–14103.

Gilson, M. K., & Honig, B. H. (1988) *Proteins 3*, 32–52.

Herron, J. N. (1984) in *Fluorescein Hapten: An Immunological Probe* (Voss, E. W., Jr. Ed.) pp 49–76, CRC Press, Boca Raton, FL.

Herron, J. N., Kranz, D. M., Jameson, D. M., & Voss, E. W., Jr. (1986) *Biochemistry 25*, 4602–4609.

Herron, J. N., He, X.-M., Mason, M. L., Voss, E. W., Jr., & Edmundson, A. B. (1989) *Proteins 5*, 271–280.

Herron, J. N., Johnston, S., Terry, A. H., He, X.-M., Voss, E. W., Jr., Guddat, L. W., & Edmundson, A. B. (1993) *Biophys. J.* (submitted for publication).

Jiskoot, W., Bloemendal, M., Van Haeringen, B., Van Grondelle, R., Beuvery, E. C., Herron, J. N., & Crommelin, D. J. A. (1991) *Eur. J. Biochem. 201*, 223–232.

Kranz, D., & Voss, E. W., Jr. (1981) *Mol. Immunol. 18*, 889–898.

Kranz, D. M., Herron, J. N., & Voss, E. W., Jr. (1982) *J. Biol. Chem. 257*, 6987–6995.

Martin, M. M., & Lindqvist, L. (1975) *J. Lumin. 10*, 381–390.

Mian, I. S., Bradwell, A. R., & Olson, A. J. (1991) *J. Mol. Biol. 217*, 133–151.

Sharp, K. A., Nicholls, A., Fine, R. F., & Honig, B. (1991) *Science 252*, 106–109.

Sturtevant, J. M. (1977) *Proc. Natl. Acad. Sci. U.S.A. 74*, 2236–2240.

Templeton, E. F. G., & Ware, W. R. (1985) *Mol. Immunol. 22*, 45–55.

Watt, R. M., & Voss, E. W., Jr. (1977) *Immunochemistry 14*, 533–541.

Wilson, I. A., Rini, J. M., Fremont, D. H., Fieser, G. G., & Stura, E. A. (1991) *Methods Enzymol. 203*, 153–177.